

Future Prospects of Spent Coffee Ground Valorisation Using a Biorefinery

Approach

Lyn Yeoh^{a,b}, Kok Siew Ng^{a*}

^aDepartment of Engineering Science, University of Oxford, Parks Road, Oxford OX1 3PJ, United Kingdom.

^bChrist Church, University of Oxford, St Aldates, Oxford OX1 1DP, United Kingdom.

Abstract

In the UK, half a million tonnes of spent coffee ground (SCG) waste are generated annually. Current SCG management practices of landfill and energy-from-waste (EfW) facilities either underutilise its valuable constituents or have negative environmental impacts. This study investigates the prospects of SCG-based biorefineries by assessing the impact of biorefinery size, location and products on economic and environmental performances. Two biorefinery design configurations are proposed. Configuration I produces biodiesel and electricity whilst Configuration II produces biodiesel and high-value chemicals. From these configurations, four biorefinery scenarios are analysed at a 10% discount rate with 2019 as the reference year. Configuration I using SCG from London coffee establishments yields a negative net present value (*NPV*) of –£3.9 million and 22% greater greenhouse gas (GHG) emissions than conventional rapeseed biodiesel production. Changing the SCG source to a coffee factory increases biorefinery size by 2.3 times but still produces a negative *NPV*. Using Configuration II to process SCG from coffee shops significantly improves *NPV*. However, without on-site energy generation, its GHG emissions are greater than those from conventional production methods of the high-value chemicals. An on-site Configuration I using SCG from the coffee factory yields the best performance. It produces a *NPV* of £3.1 million and GHG emissions 85% and 13% lower than that of SCG landfilling and conventional biodiesel. Overall, these findings demonstrate the potential of extracting value from SCG waste using a biorefinery approach, revealing a strong likelihood that future SCG biorefineries will be large scale and on-site of SCG production.

27 **Keywords:** Circular economy; spent coffee grounds; biorefinery; biofuels; techno-economic
28 analysis; carbon footprint analysis

29 * **Corresponding author.** Email: kok.ng@eng.ox.ac.uk (KS Ng)

30 **Nomenclature**

AD	Anaerobic digestion
CEPCI	Chemical Engineering Plant Cost Index
EfW	Energy-from-waste
f.o.b	Free on board
FFA	Free fatty acids
GHG	Greenhouse gas
HEN	Heat exchanger network
HMF	Hydroxymethylfurfural
IEA	International Energy Agency
OPEX	Operating expenditure
PHB	Polyhydroxybutyrate
SA	Succinic acid
SCG	Spent coffee ground
CC	Annualised capital cost (£/y)
C_{CARB}	Carbon costs from plant's net CO ₂ produced (£/y)
C_f	Cash flow in a particular year (£)
$COST_b$	Equipment cost at base size and base year (£)
$COST_f$	Equipment free on board cost at base year (£)
C_r	Equipment cost at reference year (£)
CR_E	Emissions credit from electricity exported to grid (kg CO ₂ -eq./t SCG)
CRF	Capital recovery factor
C_{RM}	Cost of raw materials (£/y)
CR_P	Emissions credit from displaced use of conventionally produced products (kg CO ₂ -eq./t SCG)
C_U	Cost of utilities (£/y)
C_{WT}	Waste treatment costs (£/y)
dr	Discount rate (%)
E_{COMB}	Emissions from combustion of biodiesel product (kg CO ₂ -eq./t SCG)
E_{ENERGY}	Emissions from energy consumed (kg CO ₂ -eq./t SCG)

EP	Economic potential (£)
E_P	Net direct CO ₂ emissions of plant (kg CO ₂ -eq./t SCG)
E_{RM}	Emissions from raw materials used (kg CO ₂ -eq./t SCG)
E_{TRAN}	Emissions from SCG transport (kg CO ₂ -eq./t SCG)
E_{WT}	Emissions from waste treatment (kg CO ₂ -eq./t SCG)
h	Annual number of operating hours (h)
IV	CEPCI Index value
N_{equip}	Total number of equipment
N_p	Total number of products
NPV	Net present value (£)
OC	Annual operating cost (£/y)
p	Base unit price of product (£/kg)
PL	Plant production lifetime (y)
r	Hourly production rate (kg/h)
R	Scaling exponent
$SIZE_b$	Equipment base size (units depend on equipment type)
$SIZE_f$	Equipment current size (units depend on equipment type)
TCC	Total capital cost (£)
VAR	Annual variable operating costs (£/y)
ΔT_{min}	Minimum temperature difference (°C)
$\Delta\%$	Percentage change in product price (%)

31

32 **1 Introduction**

33 Coffee is one of the world's most popular beverages. With a global daily consumption of 2.25
34 billion cups, its beans are second only to petroleum as an internationally traded commodity (Giller
35 et al., 2017). Coffee consumption generates large amounts of waste, with the UK alone producing
36 an estimated half a million tonnes of wet spent coffee ground (SCG) annually (Recycling Magazine,
37 2019). Currently, most SCG produced worldwide are disposed in landfills, where its decomposition
38 releases greenhouse gas (GHG) emissions into the atmosphere and acidic leachate containing
39 ecotoxic compounds (Kookos, 2018; Park et al., 2016). SCG is also treated via energy-from-waste
40 (EfW), which allows for energy recovery (Schmidt et al., 2020) but leaves the rich variety of
41 valuable organic compounds found in SCG severely underutilised. Energy recovery from SCG is

done by a company known as Bio-bean, which processes the waste into pellets or logs to be sold as renewable solid fuel (Bio-bean, 2021).

Insoluble lignocellulosic material (lignin, cellulose and hemicellulose) constitutes almost 70 wt% of dry SCG, while proteins and oils make up 11% and 15%, respectively (Obruca et al., 2015). Most SCG studies considered lignin as a fuel to deliver energy requirements (Mata et al., 2018; Saratale et al., 2020). The only SCG study found to isolate lignin was performed by Lee et al. (2019), utilising the Organosolv pre-treatment. The sugar monomers of SCG cellulose and hemicellulose have been recovered for use in microbial growth and the production of chemicals or materials (Kourmentza et al., 2018). Obruca et al. (2015) and Wang et al. (2010) found that concentrations of fermentable sugars in SCG hydrolysate can be increased through combining dilute acid hydrolysis and enzymatic digestion. Chianzy et al. (2015) investigated the application of steam explosion pre-treatment as an effective method to reduce the enzyme dosage required in the ensuing enzymatic hydrolysis of SCG. However, Mayanga-Torres et al. (2017) found that temperature above 150°C rapidly increases the formation of toxic sugar degradation products such as hydroxymethylfurfural (HMF) and furfural, which inhibit microbial activity in subsequent fermentation processes. Kovalcik et al. (2018) suggested that the removal of toxic co-contaminants present in SCG hydrolysates via detoxification steps may increase utilisation of the waste. Using different microorganism strains, the fermentation of recovered SCG sugars can yield a wide range of products, such as bioethanol, bioplastics and high-value platform chemicals (Kourmentza et al., 2018).

On average, SCG contains around 15% oil (Kondamudi et al., 2008). Synthesis of biodiesel from SCG oil via transesterification has been demonstrated (Al-Hamamre et al., 2012; Kondamudi et al., 2008), where transesterification is the reaction between triglycerides and lower alcohols. These studies used solvent extraction methods to isolate the oil from SCG. To eliminate the need for a separate oil extraction process, the *in-situ* transesterification of SCG has been investigated, where simultaneous extraction and transesterification produced biodiesel (Tuntiwiwattanapun et al., 2017).

68 However, this procedure has been criticised for its high energy consumption (Kookos, 2018). One
69 of the challenges of SCG oil transesterification arises due to its high free fatty acid (FFA) content,
70 which reacts with alkali catalysts to form soap (Tuntitiwattapun et al., 2017). To avoid
71 significant soap formation and the deactivation of the alkaline catalyst in transesterification, the
72 SCG must be of less than 3 wt% FFA (Trejo-Zárraga et al., 2018). To address this, Caetano et al.
73 (2014) performed acid esterification and alkaline transesterification on SCG oil, resulting in a 37%
74 increase in biodiesel yields when compared against the direct transesterification of SCG. Typical
75 yields of biodiesel from esterification and transesterification have been found to be around 0.84 kg
76 biodiesel/kg oil (Abdelaziz et al., 2020, 2019). Energy recovery from SCG has been explored
77 extensively in literature. Various studies showed that dried SCG has a lower heating value (18.8
78 MJ/kg at 10% moisture) greater than or comparable to conventional biomass (16.3-17.6 MJ/kg for
79 wood pellet with 7-10% moisture) but lower than fossil fuels (25-42.5 MJ/kg), and thus it is suitable
80 to be used as a fuel in direct combustion (Kang et al., 2017; McNutt and He, 2018; Mayson and
81 Williams, 2021). However, using pure SCG as boiler fuel may cause unstable combustion, leading
82 to lower boiler efficiency and elevated levels of toxic gas and particle emissions (Allesina et al.,
83 2017; Kang et al., 2017). These issues can be minimised by blending SCG with sawdust, resulting
84 in combustion parameters similar to that of wood pellets (Limousy et al., 2012). Li et al. (2014),
85 Kelkar et al. (2015), and Choi et al. (2017) investigated SCG valorisation via fast pyrolysis, which
86 involves the thermochemical decomposition of biomass into bio-oil, char, and non-condensable gas
87 at high temperatures and in an oxygen-free atmosphere. These studies demonstrated high SCG
88 conversion, with Kelkar et al. (2015) reporting SCG conversion rates of 60%, 17.7% and 20.4% for
89 bio-oil, char and pyrolysis gas when treated at 500°C and 32 seconds. A recent study by Kibret et al.
90 (2021) achieved a 95% carbon conversion at 900°C via gasification of SCG in steam and CO₂, a
91 process which also involves biomass decomposition under high temperatures. Besides that, studies
92 on the anaerobic bacterial decomposition of SCG to methane rich biogas have been performed since
93 the 1980s. This process is known as anaerobic digestion (AD). Lane (1983) and Dinsdale et al.

94 (1996) found SCG to have limited application as a mono-substrate of AD, failing to achieve stable
95 biogas production due to inhibitory compounds. To circumvent this, studies such as that by Kim et
96 al. (2016) have investigated the co-digestion of SCG with various co-substrates. As environmental
97 and resource security issues continue to rise, there has been increasing policy focus on the adoption
98 of a circular economy. Circular economy concept aims to promote reduction of resource
99 consumption and waste to landfills through reusing, recycling or converting waste materials into
100 more useful products (Department for Environment, Food and Rural Affairs (DEFRA), the
101 Department of Agriculture, Environment and Rural Affairs (DAERA), the Welsh Government and
102 the Scottish Government, 2020; Ng et al., 2019). The International Energy Agency (IEA)
103 highlighted the importance of implementing a biorefinery approach (i.e. facility with integrated
104 processes that convert biomass into value-added products) to achieve higher value generation and
105 sustainability (Ng et al., 2017; van Ree et al., 2012). It also identified the main driver of biorefinery
106 development as the efficient, cost-effective production of transportation biofuels. Furthermore, the
107 IEA proposed the production of high-value products alongside biofuel products as a promising
108 approach to reduce biofuel production costs within biorefineries (Sadhukhan et al., 2014).

109 SCG has been found to have great potential as a feedstock for the production of a wide range of
110 chemicals and materials, including biofuels (Massaya et al., 2019). However, few studies have
111 investigated the techno-economic performance of SCG biorefineries. Giller et al. (2017), Kookos
112 (2018) and Thoppil and Zein (2021) performed economic evaluations on small-scale biodiesel
113 production plants without the incorporation of high-value products. Kookos (2018) highlighted the
114 importance of large plant scales to achieve competitively priced biodiesel from SCG. The study also
115 mentioned that large scale would involve economical and practical difficulties, such as increased
116 logistical challenges and costs for SCG collection. Thoppil and Zein (2021) emphasised that
117 sensitivity analyses using different product price scenarios are needed to rigorously assess the
118 viability of producing biodiesel from SCG. There is thus a lack of literature evaluating the
119 economic and environmental performance of SCG biorefineries. These assessments are vital for

120 informing the commercial viability of SCG biorefineries and thus their future prospects (Karmee,
121 2018).

122 This study addresses the gap in literature by investigating how the economic and environmental
123 performance of SCG biorefineries are affected by the following key factors: (a) plant size; (b)
124 valorisation routes; (c) plant location relative to SCG source. Factors (a) and (b) have been selected
125 due to their significant influence on plant economics (Kookos, 2018; van Ree et al., 2012), whilst
126 (c) has been chosen to assess biorefinery economics when SCG collection costs of a large
127 biorefinery is removed by locating the plant within an instant coffee factory site. Four biorefinery
128 scenarios of different scale, valorisation routes, and locations have been analysed. The process
129 configurations focus on biodiesel production as transportation biofuels are the main drivers of
130 biorefinery development and there is a substantial amount of literature material available regarding
131 SCG valorisation to biodiesel.

132 The performances of these biorefinery systems have been compared against that of conventional
133 SCG management practices and biodiesel production processes. Additionally, the GHG emissions
134 and costs of the biorefineries have been analysed to help identify what future research efforts should
135 focus on to improve the economic and environmental performance of SCG biorefineries. The
136 novelty of this research lies in the creation of innovative conceptual biorefinery designs for SCG
137 valorisation that incorporate resource efficiency enhancement features such as multiple product
138 generation and energy integration, followed by detailed techno-economic and environmental impact
139 evaluation on different scenarios that consider plant size, valorisation routes and plant location. As
140 environmental pressure from food waste and urgency to decarbonise transport fuels escalates, this
141 research is timely and crucial to identify the most economically and environmentally compelling
142 strategies to both tackle SCG and provide society with low-carbon advanced biofuel.

143 **2 Methodology**

144 Literature review was performed to gain a holistic view of the SCG valorisation routes explored in
145 previous studies. The market values of the products from these routes, chemical composition of
146 SCG and its availability in the UK were gathered. Two biorefinery configurations were proposed.
147 As the transportation sector is a crucial driver of biorefinery development, both configurations
148 aimed to produce biodiesel. Configuration I was based on a well-researched SCG valorisation
149 pathway (i.e., transesterification) combined with current practices (i.e., incineration with energy
150 recovery). Configuration II also aimed to maximise value extracted by incorporating more novel
151 valorisation methods for the production of high-value chemicals. Four biorefinery scenarios were
152 generated, with different combinations of biorefinery size, design configuration, and location
153 relative to the SCG feedstock source. For each scenario, process simulation modelling and heat
154 integration were performed. Technical, economic, and environmental performances were then
155 evaluated using energy and mass flow data from the simulations. The key indicators used to
156 compare the scenarios include biodiesel yield, economic potential, net present value, cost of
157 production per litre of biodiesel and greenhouse gas emissions.

158 **Process Simulation Modelling:** Aspen Plus V11 software was used to simulate the mass and
159 energy flows of each system. Overall process flow diagrams were developed, with operating
160 conditions and reaction pathways established based on experimental results from literature. The
161 non-random two-liquid (NRTL) thermodynamic property method was used as non-ideal solutions
162 were simulated (Gómez-Ríos et al., 2019). Distillation columns were simulated via Aspen RadFrac
163 models with partial-vapour condensers. Pinch analysis was used to analyse the process heat
164 recovery potential and establish targets for minimum utility consumption. The mass flowrate,
165 enthalpy change, initial and final temperatures of hot and cold streams were extracted from the
166 Aspen Plus simulation results and input into Aspen Energy Analyser V11 software, along with a
167 specified global minimum temperature difference (ΔT_{min}). Using this data, a heat exchanger network
168 (HEN) design was generated and its heat exchangers used in capital and operating cost evaluations.

169 **Economic assessment:** The economic analysis involved the evaluation of capital expenditure,
 170 operating expenditure (OPEX), and profitability. An exchange rate of 1GBP = 0.72 USD was
 171 applied. The total installed capital cost (TCC) of a plant was categorised into direct and indirect
 172 costs. The direct costs included the free-on-board (f.o.b.) purchase and installation costs of the
 173 biorefinery equipment. Indirect capital costs included costs for site engineering, designing, and
 174 building. To estimate TCC , the Lang's method was used. Equipment f.o.b cost was calculated and
 175 updated to the reference year using the CEPCI index. This is shown in Equations (1)–(2), where
 176 $COST_b$ and $COST_f$ are the equipment base and purchase costs; $SIZE_b$ and $SIZE_c$ are the size capacities of
 177 the base and current systems; R is the scaling exponent; C_r is the cost; IV_r and IV_b the index values
 178 of the reference year (2019) and base year (Davis et al., 2013). Finally, TCC was calculated using
 179 Equation (3), where N_{equip} is the total number of equipment and 5.03 is the Lang factor of a solid-
 180 fluid processing biorefinery (Sadhukhan et al., 2014). This method of estimating capital investment
 181 gives a 30% accuracy. However, it must be noted that the investment required for a new plant on an
 182 undeveloped site will be larger than on an existing, developed site. The annualised capital cost (CC)
 183 was obtained by spreading TCC over the plant's lifetime (PL) of 20 years at a discount rate (dr) of
 184 10%, which is similar to the discount rates used in previous biorefinery economic analyses
 185 (Zetterholm et al., 2020). CC was estimated by using a capital recovery factor (CRF) as in
 186 Equations (4)–(5) (Ng and Martinez-Hernandez, 2020).

$$\frac{COST_f}{COST_b} = \left(\frac{SIZE_c}{SIZE_b} \right)^R \quad (1)$$

$$C_r = COST_f \left(\frac{IV_r}{IV_b} \right) \quad (2)$$

$$TCC = 5.03 \times \sum_{i=1}^{n=N_{equip}} C_{r,i} \quad (3)$$

$$CRF = \frac{dr(1+dr)^{PL}}{(1+dr)^{PL}-1} \quad (4)$$

$$CC = TCC \times CRF \quad (5)$$

188 OPEX included fixed and variable operating costs. Fixed operating cost comprised of the costs of
 189 labour, supervision, laboratory, plant overhead, maintenance, local taxes and insurance (see
 190 Appendix B, Table B.1). The number of personnel needed per shift was calculated by multiplying
 191 the number of plant processing steps with the number of personnel required per step. The annual
 192 cost of labour was calculated using Equation (6). The annual variable operating cost of the plant
 193 (VAR) [£/y] was calculated using Equation (7), where C_{RM} [£/y] represents raw material cost, C_U
 194 [£/y] the utilities cost, C_{WT} [£/y] the waste treatment costs and C_{CARB} [£/y] the carbon costs based on
 195 the plant's net flowrate of CO₂. Economic viability was measured using key performance
 196 indicators such the economic potential (EP) [£], net present value (NPV) [£] and payback period.
 197 EP and NPV were calculated using Equations (8)–(9), where h [h] is the number of operating hours
 198 annually; r_i [kg/h] and p_i [£/kg] are the production rate and base unit price of product i respectively;
 199 N_p is the total number of products; OC [£/y] is the annual operating costs and C_f [£] refers to the
 200 cash flow in a particular year (Ng et al., 2013).

$$\text{Cost of personnel (\pounds/year)} = \text{Number of personnel per shift} \times 5 \text{ shifts} \times 40 \text{ hours/week} \times \frac{1}{52 \text{ weeks/year}} \times \text{Hourly wage} \quad (6)$$

$$VAR = C_{RM} + C_U + C_{WT} + C_{CARB} \quad (7)$$

$$EP = h \sum_{i=1}^{i=N_p} r_i p_i - CC - OC \quad (8)$$

$$NPV = \sum_{n=0}^{n=PL} \frac{C_f}{(1+dr)^n} \quad (9)$$

201

202 **Environmental impact assessment:** The system boundary was defined (see Figure 1) and
 203 inventory analysis was performed.

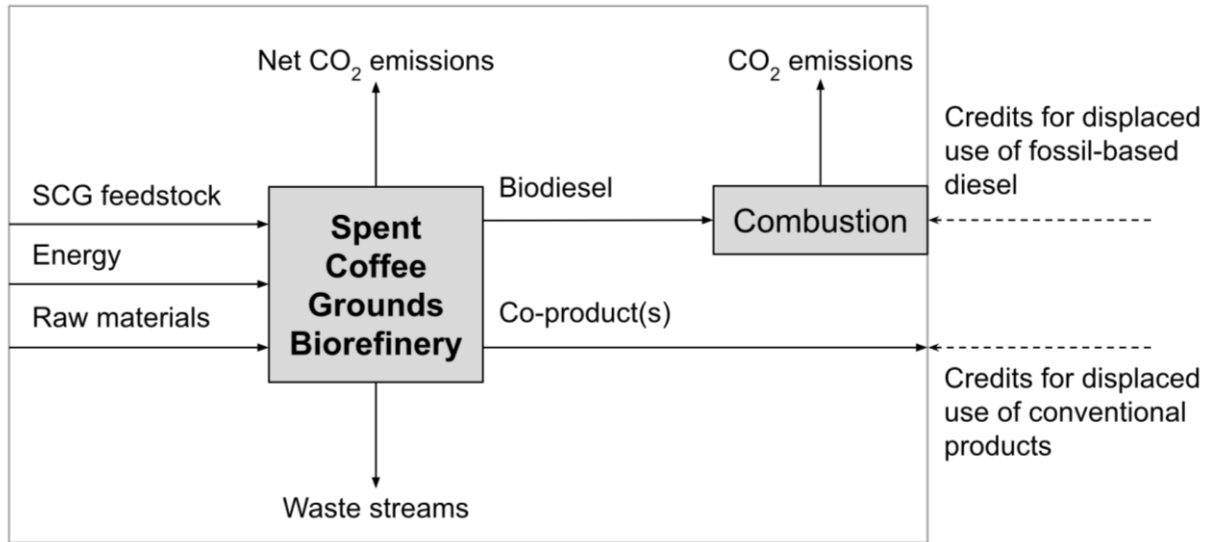


Figure 1. System boundary for the SCG biorefinery.

Input and output stream data were compiled from simulation results. CCaLC2 (a life cycle assessment software developed by the University of Manchester) was used to estimate the GHG emissions of these input and output flows. Using ISO 14067 standards (International Organization for Standardization, 2018), the net GHG emissions of the SCG biorefinery was calculated using Equation (10), where E_{RM} , E_P , E_{COMB} , E_{ENERGY} , E_{TRAN} , E_{WT} are the emissions from the raw materials used, the plant processes, the combustion of the biodiesel produced, the energy consumed, SCG transport, and waste treatment. Emission credits (GHG removals) for the electricity exported to the grid (CR_E) and displacement of conventional production of the products generated from SCG (CR_P) are applied.

$$\text{Net GHG} = E_{RM} + E_P + E_{COMB} + E_{ENERGY} + E_{TRAN} + E_{WT} - CR_E - CR_P \quad (10)$$

Sensitivity analysis: Price sensitivity analysis was performed on all scenarios using methodology outlined by Ng et al. (2013). A percentage change in price ($\Delta\%$) was defined and three sets of prices were generated for each product: the base price (subscript 0), a price $\Delta\%$ lower than the base price (subscript $-\Delta\%$), and a price $\Delta\%$ higher than the base price (subscript $+\Delta\%$). For Np number of products, there are n possible combinations of prices. MATLAB was used to calculate the revenues of each of these combinations using the equation shown in Equation (11), where the price scenarios matrix was multiplied by production rates (r) to give n revenue scenarios. The capital and operating

costs (assumed to be fixed) were subtracted from each element of the revenue column vector produced in Equation (11) to give the *EP* for each price scenario.

An economic risk is a change in revenue due to change in the combination of product prices. Classes of economic risks were defined in terms of the percentage change in *EP* relative to the *EP* calculated from base prices. The probability of a class of economic risk occurring is the ratio of the number of combinations that produce that class of economic risk to the total number of combinations.

$$\begin{bmatrix} p_{1,0} & p_{2,0} & \cdots & p_{Np,0} \\ p_{1,+\Delta\%} & p_{2,+\Delta\%} & \cdots & p_{Np,+\Delta\%} \\ p_{1,-\Delta\%} & p_{2,-\Delta\%} & \cdots & p_{Np,-\Delta\%} \\ \vdots & \vdots & \vdots & \vdots \end{bmatrix}_{n \times Np} \begin{bmatrix} r_1 \\ r_2 \\ \vdots \\ r_{Np} \end{bmatrix}_{Np \times 1} = \begin{bmatrix} p_{1,0} r_1 + \cdots + p_{Np,0} r_{Np} \\ p_{1,+\Delta\%} r_1 + \cdots + p_{Np,+\Delta\%} r_{Np} \\ p_{1,-\Delta\%} r_1 + \cdots + p_{Np,-\Delta\%} r_{Np} \\ \vdots \end{bmatrix}_{n \times 1} \quad (11)$$

3 SCG Biorefinery Configurations: Modelling and Integration

This section details the two biorefinery configurations proposed. Process description and mass and energy balances are presented. Detailed stream tables, process flowsheets and the specifications used in Aspen Plus process models are provided in Appendix C.

3.1 Proposed SCG Configurations

In the biorefinery configuration descriptions, a wet SCG plant input of flowrate 5767 kg/h at 20°C was employed based on SCG produced by London coffee establishments (see Section 3.2). Configuration I produces biodiesel from extracted SCG oil, with electricity generated as a co-product due to the combustion of defatted SCG. Heat from the combustion is exported to a heat network. Configuration II produces biodiesel as well as succinic acid (SA), aromatics (vanillin, vanillic acid, guaiacol, acetovanillone), carboxylic acids (formic acid, acetic acid) and polyhydroxybutyrate (PHB) bioplastic. In contrast to Configuration I, no combustion is performed. Heat integration in both configurations uses a ΔT_{min} of 15°C.

244 3.2 SCG Feedstock

245 **SCG feedstock composition:** SCG feedstock was modelled with a moisture content of 66%
 246 (Caetano et al., 2014). Dry mass compositional data and their representative Aspen Plus
 247 components are presented in Table 1 (Obruca et al., 2015). Further details about the component data
 248 used in the simulations can be found in Table A.1 of Appendix A.

249 Table 1. Chemical composition of SCG dry mass and the representative components adopted in
 250 Aspen Plus (Obruca et al., 2015).

SCG Component	Representative component adopted in Aspen Plus	Content ⁽ⁱ⁾ (wt%)
Cellulose	Cellulose	10.95
Hemicellulose	Cellulose	31.83
Lignin	Vanillin	27.00
Oil (triglycerides)	Triolein	11.35
Oil (free fatty acids)	Oleic acid	3.65
Protein ^(iv)	Glutamic acid ⁽ⁱⁱ⁾	10.70
Polyphenol	Caffeic acid ⁽ⁱⁱⁱ⁾	2.50
Caffeine	Caffeine	0.02
Ash ^(iv)	Calcium Oxide	2.00
Moisture	Water	66

251

252 Note:

253 ⁽ⁱ⁾ All components are in wt% of dry mass except for water.

254 ⁽ⁱⁱ⁾ Glutamic acid found to be major component of SCG protein (Martinez-Saez et al., 2017).

255 ⁽ⁱⁱⁱ⁾ Caffeic acid identified in SCG (Panusa et al., 2013).

256 ^(iv) Protein and ash treated as insoluble compounds and did not partake in any chemical reaction (Humbird et al., 2011).

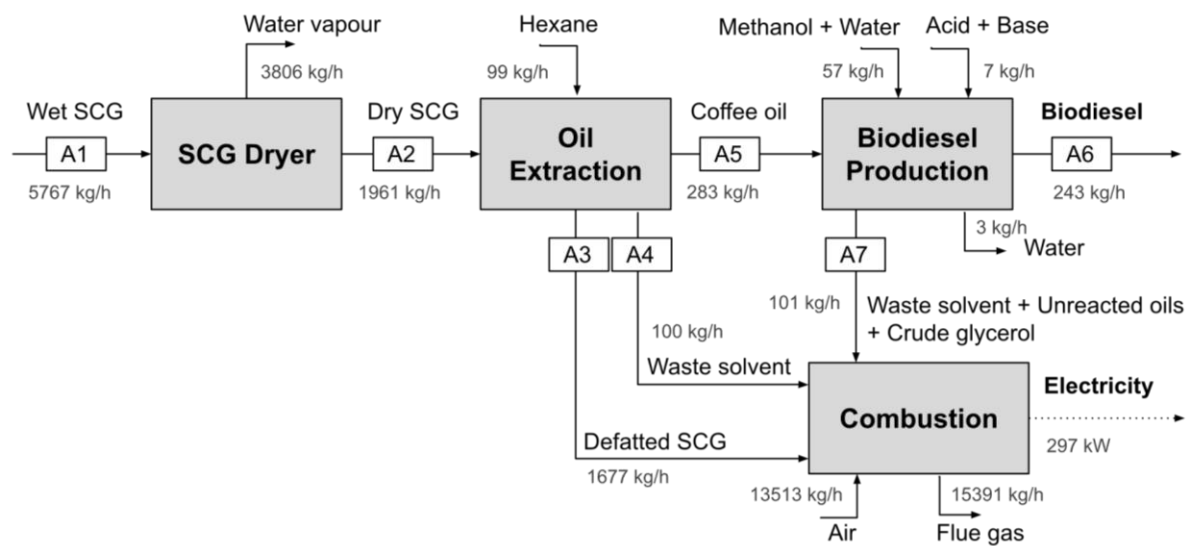
257 **SCG feedstock availability:** The SCG used in the scenarios was obtained from either London
 258 coffee establishments or Nestlé's coffee factory in South Derbyshire, UK. The parameters used to
 259 calculate the amount of SCG produced in London coffee shops are summarised in Table A.3 of
 260 Appendix A. The total amount of wet SCG produced in London coffee establishments was
 261 calculated using Equation (A.1), giving a value of 46,136 t/y. On the other hand, the annual wet
 262 SCG production rate from Nestlé's coffee factory was calculated as 105882 t/y using Equation
 263 (A.2) and the parameters in Table A.4.

264 **3.3 Biorefinery Scenarios**

265 This section outlines four SCG biorefinery scenarios based on Configurations I and II, described in
266 Sections 3.5 and 3.5. The biorefinery plants in Scenarios A, B and D were taken to be 70 km away
267 from their SCG source, based on the average distance between the centre of Greater London and its
268 perimeter. Other parameters used for SCG transport are included in Table A.2 in Appendix A.
269 Besides this, input SCG feedstock of these 3 scenarios enters the biorefineries at 20°C. Scenario A
270 is considered the base case scenario. Here, Configuration I processes all the SCG generated in
271 London coffee shops, producing biodiesel and electricity. The parameters used in Scenario B are
272 identical to those of Scenario A except for the use of all the SCG produced from the Nestlé coffee
273 factory. On the other hand, Scenario C assumes the biorefinery of Scenario B is located within the
274 coffee factory site and that the SCG is delivered directly from the factory's coffee brewing process,
275 entering the biorefinery at 80°C. SCG transportation is excluded in Scenario C and the SCG
276 feedstock is thus obtained at no cost. Scenario D uses parameters identical to that of Scenario A
277 apart from the use of Configuration II.

278 **3.4 Configuration I**

279 The flow diagram is illustrated in Figure 2.



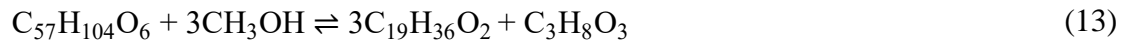
281

282 Figure 2. Flow diagram of SCG biorefinery Configuration I.

283 **SCG drying and oil extraction:** Wet SCG (stream A1) is dried at 102°C to reduce moisture
284 content from 66% to 0%. As moisture reduces oil solubility in the hydrophobic solvent, the absence
285 of water is crucial to achieve high oil extraction yields in the following process (Najdanovic-Visak
286 et al., 2017). Solvent extraction of the SCG oil content (FFAs and triglycerides) is performed on dry
287 SCG (stream A2) at 60°C, with process parameters summarised in Table C.1 of Appendix C
288 (Najdanovic-Visak et al., 2017). *n*-hexane is used as it has been found to give the highest yield of
289 oil (Somnuk et al., 2017). The liquid solvent/oil mixture and the solid defatted SCG are separated
290 via centrifugation and the solvent is removed in a flash vessel at 0.1 bar and 80°C. The separated
291 solvent is recycled for further use in oil extraction. The defatted SCG (stream A3) and waste solvent
292 stream from the recycle loop purge (stream A4) are combusted whilst the extracted coffee oil
293 (stream A5) is used in biodiesel production.

294 **Biodiesel production from SCG oil:** Oil (stream A5) enters a two-step process to produce
295 biodiesel (Efthymiopoulos et al., 2018; Hochegger et al., 2019; Saratale et al., 2020). Esterification
296 is performed before transesterification to esterify the FFA and minimise soap formation. Table C.2
297 summarises the process parameters used. During the esterification process described in Equation
298 (12), methanol (CH₃OH) reacts with FFA (C₁₈H₃₄O₂) to form biodiesel (C₁₉H₃₆O₂) with sulphuric

299 acid as the catalyst. The products of esterification undergo sodium hydroxide (NaOH) catalysed
 300 transesterification where biodiesel and glycerol (C₃H₈O₃) are formed, as shown in Equation (13).



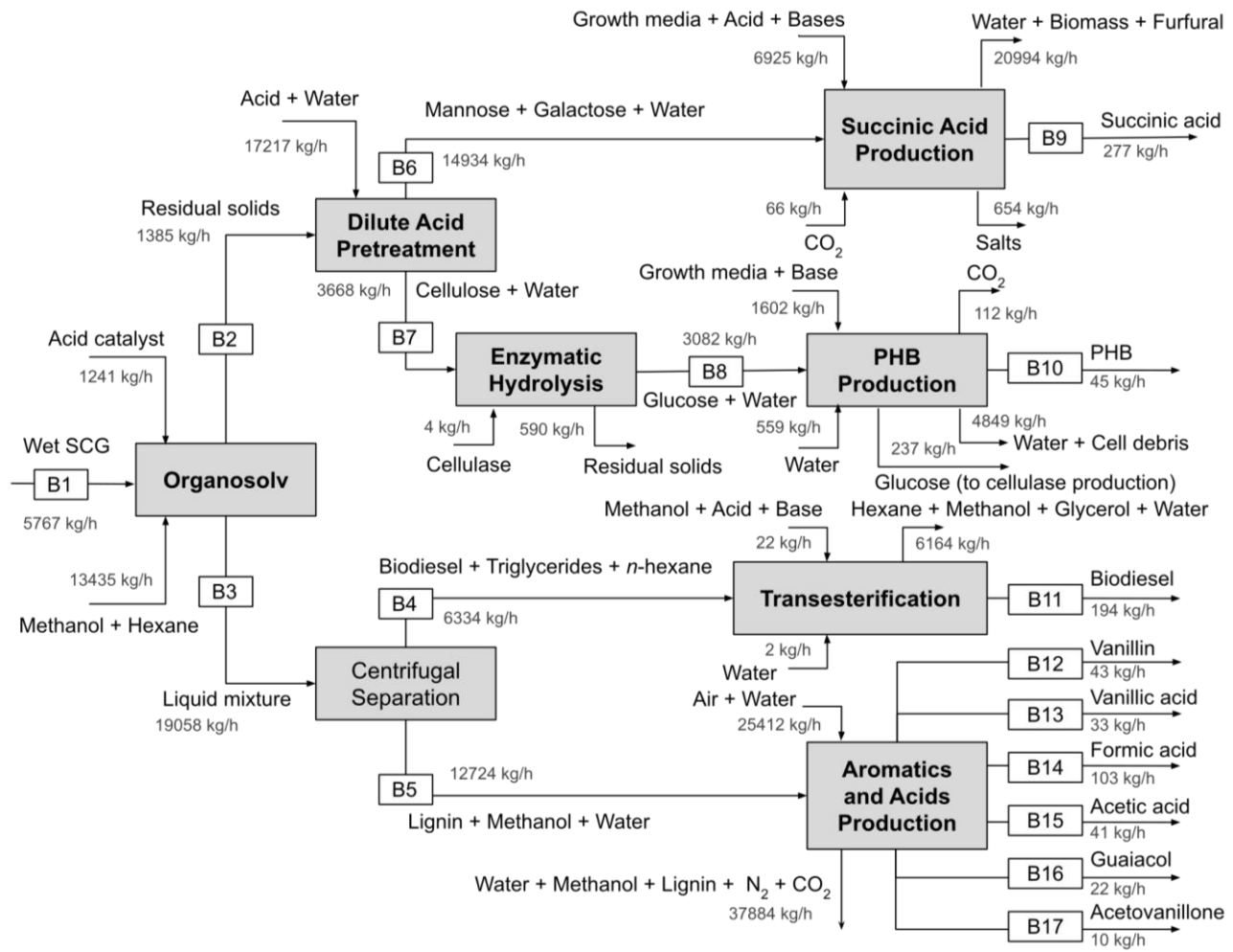
301 The transesterification products enter a flash vessel at 162°C and 1 bar to recover methanol for
 302 recycling. The bottom products of the flash vessel are washed in acidic water to neutralize the base
 303 catalyst used in transesterification. Next, centrifugation separates biodiesel, methanol, and hexane
 304 from the other denser liquids. Two flash vessels at 0.1 bar and 167°C and 270°C purify the
 305 biodiesel, producing biodiesel (stream A6) to EN14214 European standards (Tsoutsos et al., 2019).
 306 The crude glycerol produced from transesterification, methanol recycle-loop purge and other waste
 307 organic streams consisting of unreacted oils (stream A7) are combusted.

308 **Combustion of defatted SCG and waste streams:** The combustion of streams A3, A4 and A7 was
 309 modelled using a stoichiometric reactor at 500°C and 1 bar. Flue gas exiting the combustion
 310 chamber at 500°C is used to pre-heat boiler feed water from 20°C to 102°C, reducing the gas
 311 temperature to 112°C. The heat from combustion reactor is used to generate steam of 480°C and
 312 135 bar from the pre-heated water. The steam drives a turbine of 90% isentropic efficiency and a
 313 pressure drop of 107.5 bar, generating a total of 1085 kW of electricity. Of this, 788 kW is used by
 314 plant processes and the remaining 297 kW is exported to the grid. Heat from the steam leaving the
 315 turbine (247°C and 27.5 bar) and the flue gas (112°C) is extracted and exported to a heating
 316 network. The flue gas contains 3528 kg/h of CO₂, of which 86% is due to the combustion of SCG
 317 material.

318 **Validation of simulation results:** In this configuration, 5767 kg/h of SCG at 66% moisture
 319 produces 283 kg/h of oil and 243 kg/h of biodiesel product. This corresponds to a yield of 0.86 kg
 320 biodiesel per kg coffee oil, which is in close agreement with the average of yields found from
 321 literature, i.e. 0.84 kg biodiesel/kg oil (Abdelaziz et al., 2020, 2019).

322 **3.5 Configuration II**

323 The process block diagram was illustrated in Figure 3.



324
325 Figure 3. Flow diagram of SCG biorefinery Configuration II.

326 **Pre-treatment:** To isolate lignin, Organosolv pre-treatment was selected as it is the only
327 experimentally validated technique of SCG lignin isolation found in literature (Lee et al., 2019).
328 The process conditions used are adopted from said study. The wet SCG feedstock (stream B1) does
329 not undergo pre-drying as the high moisture content promotes solvent penetration into SCG during
330 pre-treatment, therefore increasing delignification rates (Hochegger et al., 2019).

331 Solvents *n*-hexane and methanol are added to a reactor at 161°C and 1 bar, along with sulphuric
332 acid as the catalyst. Under these conditions, lignin dissolves in methanol, while triglyceride and
333 FFA are simultaneously extracted into *n*-hexane. The sulphuric acid catalyses the esterification of
334 the extracted FFA, forming biodiesel. The solid residues consisting of mainly hemicellulose and

cellulose fibres are removed using a filter, forming stream B2. The remaining liquid mixture (stream B3) is separated into stream B4 (containing solubilised lignin) and stream B5 (containing mainly biodiesel and triglycerides) via centrifugation. Lignin and biodiesel recoveries of 56% and 62.4% are obtained from the Organosolv reactor (Lee et al., 2019). Oil extraction yield was taken as 78 wt% (Efthymiopoulos et al., 2018).

Dilute acid pre-treatment and enzymatic hydrolysis: The solid residues of stream B2 are slurried in dilute sulphuric acid and treated at 163°C and 1 bar (Mussatto et al., 2011). Under these conditions, hemicellulose is converted to its monomeric sugars. After pre-treatment, the solid cellulose and hemicellulose hydrolysate are separated via centrifugation, after which the solids are washed with water to remove any residual soluble sugars and fermentation inhibitors (sugar degradation products). The water stream from this washing stage is merged with the hemicellulose hydrolysate and the resulting stream is detoxified using a granular activated carbon column to remove HMF and furfural formed (Nieder-Heitmann et al., 2019). The column output stream is sent to a neutralisation reactor (38°C, 1 bar) where calcium hydroxide neutralises the remaining acid. The resulting salt is precipitated and filtered out, leaving a hemicellulose sugar-rich stream (stream B6) utilised in SA production. On the other hand, the solid cellulose residues (stream B7) from the dilute acid pre-treatment are subjected to enzymatic hydrolysis at 48°C. Here, cellulase enzymes convert the cellulose fibres into glucose monomers and small traces of soluble gluco-oligomers. Solid residues of unreacted lignin, proteins, cellulose, and other compounds are removed from the aqueous glucose stream (stream B8) via centrifugation.

SA production from hemicellulose: The detoxified, neutralised aqueous solution of hemicellulose sugars (stream B6) is utilised in SA production using the bacteria *Actinobacillus succinogenes* (Nieder-Heitmann et al., 2019). Like PHB production, growth and synthesis reactors are used. Both reactors operate at 38°C. With 10% of stream B6 directed to the growth reactor, the remaining is sent to the synthesis block, after passing through flash drums to concentrate the hydrolysate stream to 200 g/L of sugars (Nieder-Heitmann et al., 2019).

361 The products of the synthesis reactor are filtered to remove cells and the liquid product stream sent
362 to an adsorption tower. An adsorption tower using resin NERCB 09 is used due to its high SA
363 selectivity and average recovery of 96% (Li et al., 2009). After adsorption, the adsorbent is easily
364 regenerated using NaOH solution. As SA reacts with the base to form sodium succinate, sulphuric
365 acid is added to the reactor, forming sodium sulphate and SA. A patented process involving
366 selective precipitation of sodium sulphate is applied to recover the SA (Fujita and Wada, 2008).
367 Finally, a distillation column removes water, producing the SA product stream B9.

368 **PHB production from cellulose:** A fraction of the glucose-rich stream B8 is diverted as feed for
369 the cellulase production plant at a rate of 3.9 kg/h of glucose per kg/h of cellulase required
370 (Humbird et al., 2011). The remaining glucose is used for PHB production. Although there exists a
371 variety of microbes with the ability to produce PHB intracellularly, the use of recombinant *E. coli*
372 was chosen as it produces PHB during both growth and synthesis phases, resulting in lower
373 residence times and capital costs (Nieder-Heitmann et al., 2019). The PHB production process
374 consists of growth and synthesis phases, product separation and purification. The glucose stream
375 from the enzymatic hydrolysis of cellulose is split into two streams, with 9.5% sent to the growth
376 reactor and the remaining to the synthesis reactor. Before these glucose streams enter the reactors,
377 they are either mixed with water or undergo evaporation to achieve glucose concentrations of 20
378 g/L and 700 g/L for the growth and synthesis reactors, respectively. The growth reactor produces a
379 population of microorganisms from a stock dormant culture, sugar, and ammonia for use in PHB
380 production in the synthesis reactor. The microbial cells are sent to the synthesis reactor, where
381 concentrated glucose (700 g/L) is fed for continued bacterial growth and intracellular PHB
382 production. A centrifuge separates the cells containing PHB from the fermentation broth. After a
383 water wash at 30°C, the cells are lysed in a blending tank at 30°C containing a 0.2 M NaOH
384 solution to release the PHB within the cells. The PHB crystallises upon exposure to the solution
385 (Nieder-Heitmann et al., 2019). Finally, the crystalline PHB is subjected to a final water wash and

centrifugation to remove any residual cell material before being atomized into particles using a spray dryer, forming stream B10.

Biodiesel production from oil: Stream B4 is subjected to identical transesterification and biodiesel purification processes as in Configuration I. However, *n*-hexane is first separated from the lipids using a flash drum at 75°C and 0.06 bar. Biodiesel (stream B11) is produced.

Production of aromatic compounds and acids from lignin: The soluble lignin of stream B5 is precipitated out via the addition of water and the solid lignin formed is separated using a filter. This lignin and compressed air enter an oxidative depolymerisation reactor (160°C, 8 bar) (Fujita and Wada, 2008; Li et al., 2009) where lignin reacts with oxygen to produce vanillin, vanillic acid, formic acid, acetic acid, guaiacol, and acetovanillone (streams B12-B17), along with CO₂. Unreacted lignin is removed via filtration and recycled back to the depolymerisation reactor to maximise production of the high-value chemicals. The products in the liquid stream are isolated using a novel hydrophobic membrane separator that has been shown to achieve perfect separation of organic and aromatic compounds from aqueous mixture (IEA Bioenergy, 2021; Phillips et al., 2019). The membrane unit thus was modelled using a separator block with perfect separation of organic compounds. The products in the organic phase output stream of the membrane separator are separated using a series of distillation columns under vacuum conditions to give product streams B12-B17 of 98-99% purity.

404

4 Results and Discussion

The parameters and assumptions used in the scenarios were outlined in Section 4.1. Performance analyses explored the influence of size, location and products on the economic and environmental performance of a biorefinery, presented in Section 4.2. The biorefinery GHG emissions were compared against that of conventional SCG management practices. Biorefinery performances were

also compared against that of conventional biodiesel. Section 4.3 provides insights on the future prospects of SCG biorefineries and recommendations for future studies.

4.1 Parameters and Assumptions for Scenarios

Parameters for performance evaluation: To determine economic performance, h was taken as 8000 hours. For labour cost calculations (Equation (6)), Configuration I involved 3 processing steps and was considered automated, requiring one personnel per step. Configuration II had 6 processing steps, with 3 personnel required per step due to the complexity of the plant design. The EP and NPV were calculated using Equations (8)–(9), where the values of Np were 3 and 9 for Configuration I and II respectively. Price sensitivity analysis was performed (see Section 2) with price fluctuations ($\Delta\%$) of 10%. The unit product prices are summarised in Table D.1 of Appendix D. The cost of production of biodiesel (£/L) was calculated using Equation (14).

$$\text{Biodiesel cost} = \frac{\text{Total annual production cost}}{\text{Litres of biodiesel produced annually}} \times \frac{\text{Biodiesel revenue}}{\text{Total revenue}} \tag{14}$$

Net GHG values were calculated using Equation (10) and net heat and electricity consumptions were calculated by subtracting heat and electricity consumed from that produced by SCG combustion.

4.2 Performance Analysis

The parameters and key performance indicators of each scenario are summarised in Table 2, where negative values of net heat or electricity consumption represents net generation and subsequent export to heat networks or the electrical grid.

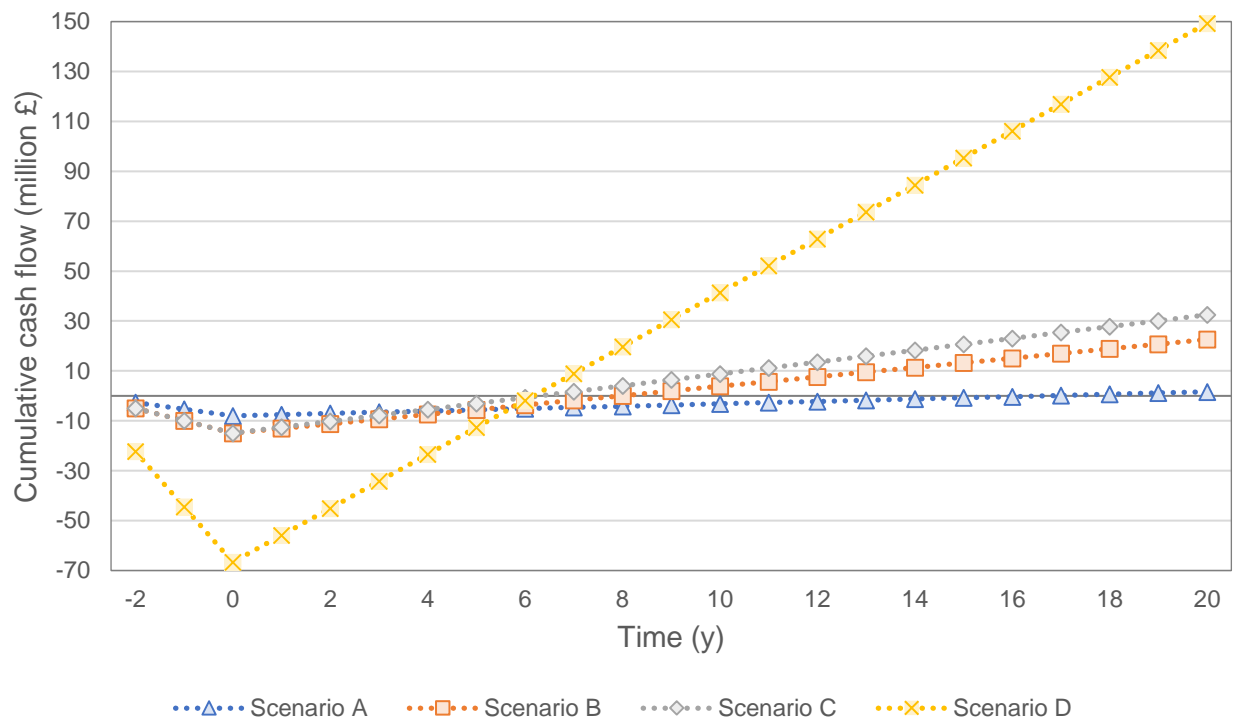
Table 2. Parameters and key performance indicators of the scenarios analysed.

	Scenario A	Scenario B	Scenario C	Scenario D
Brief Description	Config I London SCG Off-site	Config I Factory SCG Off-site	Config I Factory SCG On-site	Config II London SCG Off-site
Parameters				
Configuration	I	I	I	II

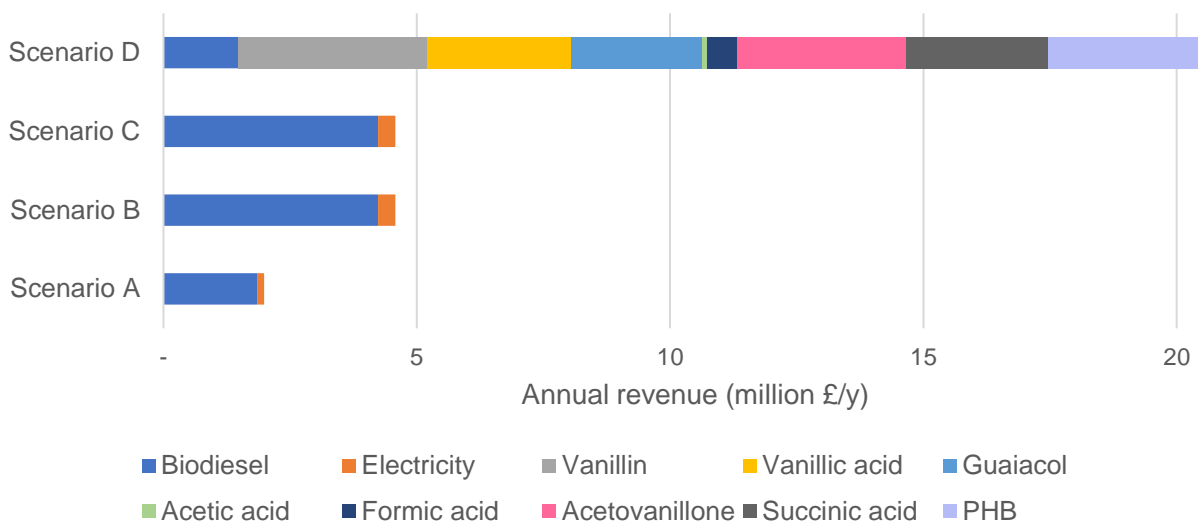
SCG feedstock source	London shops	Nestlé factory	Nestlé factory	London shops
SCG transport distance (km)	70	70	-	70
SCG feedstock temperature (°C)	20	20	80	20
SCG feedstock flowrate (t/y)	46136	105882	105882	46136
Technical Performance Indicators				
Biodiesel yield (kg biodiesel/t SCG processed)	42.10	42.10	42.10	33.60
Net heat consumption (MJ/t SCG processed)	– 3392.93	–3501.58	–3522.28	7575.38
Net electricity consumption (MJ/t SCG processed)	–185.12	–195.01	–195.01	144.84
Economic Performance Indicators				
Economic potential, <i>EP</i> (million £/y)	–0.46	0.12	0.62	2.97
Net present value, <i>NPV</i> (million £)	–3.90	–0.42	3.07	15.19
Payback period (y)	16.6	8.0	6.3	6.2
Cost of biodiesel production (£/L)	1.02	0.81	0.72	0.69
Environmental Performance Indicators				
GHG emissions (kg CO ₂ -eq./t SCG processed)	81.21	80.98	78.61	2233.00

429

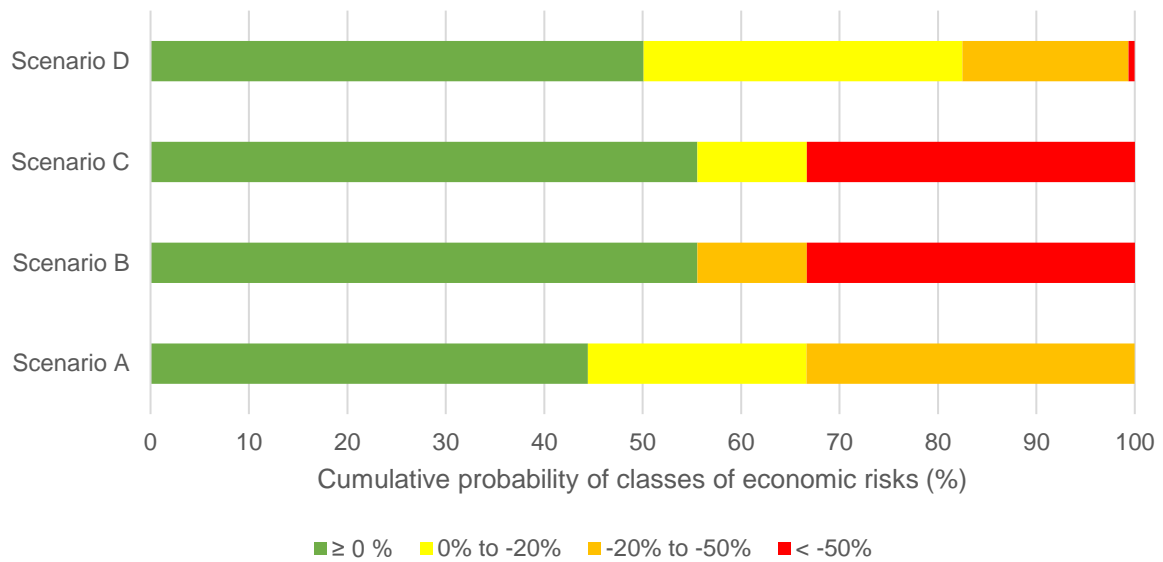
430 Figure 4 presents the economic and environmental performance of the scenarios. The cumulative
431 cash flows of the scenarios are illustrated in Figure 4 (a), where *TCC* is evenly divided between
432 years –2 to 0. Positive and negative *NPV* values indicate profitable and loss-making projects,
433 respectively. The payback periods of Table 2 are the number of years required to recover the *TCC*
434 investment. These are represented by the x-axis intercepts on Figure 4 (a) and are a measure of the
435 plant’s attractiveness as an investment. Revenues are categorised by product sales in Figure 4 (b)
436 and cost breakdowns of the scenarios are shown in Figures D.1–D.3. The results of the price
437 sensitivity analysis are illustrated in Figure 4 (c), with the legend indicating the classes of economic
438 risk. For example, ‘0 to –20%’ economic risks referred to price combinations that resulted in a 0 to
439 20% decrease in *EP* relative to the *EP* generated from base prices. For Scenario A, none of the price
440 combinations resulted in a positive value for *EP*, while all the price combinations of Scenarios C
441 and D generated positive *EP*.



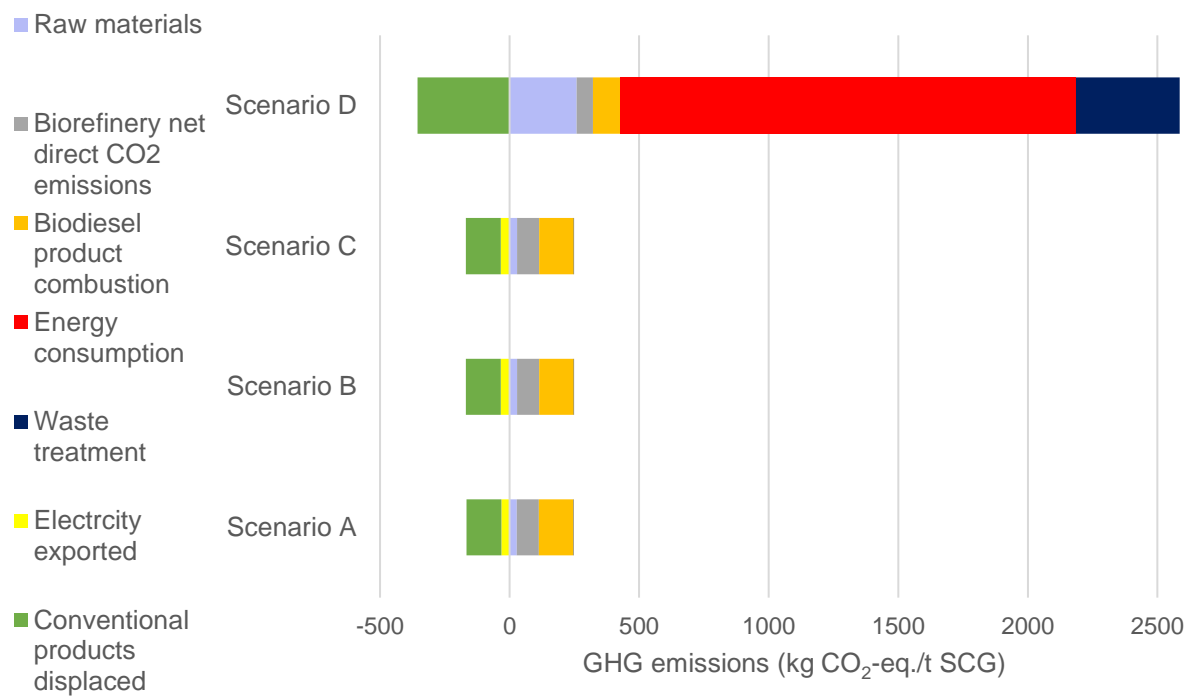
(a)



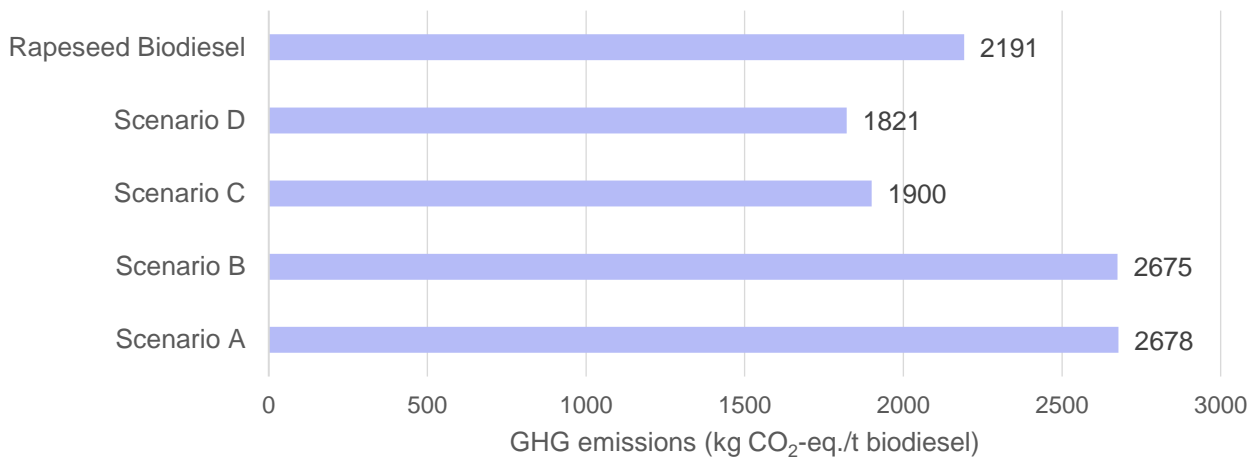
(b)



(c)



(d)



(e)

Figure 4. Economic and environmental performance of scenarios analysed. (a) Cumulative cash flows for the plant's 20 years of operation; (b) Classification of revenues by product sales; (c) Likelihood of different classes of economic risk; (d) Classification of GHG emissions per tonne of SCG processed; and (e) GHG emissions per tonne of biodiesel produced.

Plant size: The impact of increasing biorefinery size was investigated by comparing the performances of Scenario A and B, with SCG feedstock flowrates of 46136 and 105882 t/y, respectively. Scenario A generates a negative *NPV* value of −£3.9 million, implying that this scenario is not economically compelling. Increasing the plant size by 2.3 times to that of Scenario B still resulted in an economically unviable plant, with a *NPV* of −£0.42 million (Table 2). However, the increase in *NPV* along with the reduction in payback period from 16.6 to 8.0 years (Figure 4 (a)) indicates that Scenario B is a more attractive investment than Scenario A. The cost of biodiesel production was reduced by 18% from 0.88 to 0.72 £/L (Table 2). This improved economic performance aligns with previous hypotheses that larger scale of SCG biorefineries is required to result in an economically viable production (Giller et al., 2017). Besides that, a price sensitivity analysis of both scenarios (Figure 4 (c)) reveals that Scenario B has a 11% greater likelihood of $\geq 0\%$ economic risks when product prices fluctuate from their base levels. A $\geq 0\%$ economic risk refers to an increase or no change in *EP* relative to the *EP* generated at base prices, thus requiring no modification to the biorefinery processes. The likelihood of $< -50\%$ economic risks rose from

0% (Scenario A) to 33% (Scenario B). This type of economic risk would greatly reduce *NPV* and thus would require plant process modifications to minimise its large negative economic impact. Generally, the greater the likelihood of $< -50\%$ economic risks, the higher the economic risk of the scenario. Thus, increasing the biorefinery size results in an overall rise in the plant's economic risk. On the other hand, environmental performance (see Figure 4 (d)) does not improve by increasing biorefinery size, with the GHG emissions of Scenario B a mere 0.3% lower than that of Scenario A. Biodiesel yield per tonne of SCG processed is not affected while the net heat and electricity generated per tonne of SCG increase with biorefinery size.

Biorefinery location: Scenarios B and C were compared to examine the impact of biorefinery location relative to the SCG source. Locating the biorefinery within Nestlé's Derbyshire coffee factory site results in significant improvement in economic performance, with *NPV* growing by 9.3 times to £3.1 million, a 1.7-year reduction in payback period and a 11.1% reduction in biodiesel production cost. These findings demonstrate the significance of a centralised processing facility on the economic performance of SCG valorisation, as concluded by Kookos (2018). Economic risk also decreases, with around a tenth of price combinations generating economic risks of 0% to -20% instead of -20% to -50% . However, there remains a 33% likelihood that 10% product price fluctuation results in $< -50\%$ economic risk, indicating that the economic viability of Scenario C is still vulnerable to market price fluctuations. Besides that, the omission of SCG transport results in a 30% reduction in raw material cost and a 3% reduction in GHG emissions. While biodiesel yield and net electricity consumption remain unchanged, net heat generated increases slightly by 0.5% as the SCG feedstock enter at 80°C , resulting in lower SCG drying heat requirements.

Biorefinery products: The impact of producing high-value chemicals was assessed by comparing Scenarios A and D. Scenario D has excellent economic performance, with a *NPV* of £15.2 million and a payback period of 6.2 years. The cost of biodiesel production decreases by 4% from 0.72 £/L to 0.69 £/L due to biodiesel comprising a much smaller proportion of total revenue and use of

Equation (14). This result supports the IEA's proposition that producing high-value products alongside biofuels would lower biofuel production costs (van Ree et al., 2012). As illustrated in Figure 4 (b), almost 90% of the annual revenue generated by Scenario D is evenly distributed between sales from vanillin, vanillic acid, guaiacol, acetovanillone, SA and PHB. This even distribution of revenue across many products leads to the reduced economic risk seen in the results of the sensitivity analysis in Figure 4 (c). In contrast, Scenario A has much higher economic risk due to biodiesel sales constituting 93% of its revenue. Thoppil and Zein (2021) also found the *NPV* of SCG biorefinery to be highly sensitive to product prices when products are of limited range and low value.

However, the economic performance of Scenario D is at the cost of greater environmental impact, with GHG emissions increasing by 27.5 times to 2233 kg CO₂-eq./t SCG (Figure 4 (d)). Steam generation and electricity usage constitute 52% and 18% of the total emissions from the plant, respectively. These emissions have been grouped and labelled as 'energy consumption' in Figure 4 (d). For its GHG emissions/t SCG to match that of Scenario A, the energy consumption of Scenario D would have to be reduced by at least 22%. As Scenario D does not involve on-site energy recovery via combustion, it results in net electricity and heat consumption 3.2 and 1.8 times that of Scenario A. Besides that, Scenario D results in a biodiesel yield around 20% less than Scenario A due to the lower biodiesel yields of the Organosolv pre-treatment.

Conventional SCG management practices: The environmental impacts of Scenarios A and D were compared against that of the two most widespread SCG management practices in the UK: EfW and landfilling. Schmidt et al. (2020) found the GHG emissions of SCG EfW and landfill facilities with energy recovery to be -435 kg CO₂-eq./t SCG and 525 kg CO₂-eq./t SCG, respectively. Neither Scenario A nor D have GHG emissions as low as EfW practices. Scenario A produces around 85% less GHG emissions than landfilling while Scenario D produces more than 4 times the GHG emissions of landfilling. Note that Scenarios B and C were excluded from this comparison due to the similarity of their GHG emissions with that of Scenario A.

522 **Conventional biodiesel production:** The GHG emissions of Scenarios A to D were compared
 523 against that of conventional biodiesel production in Europe. Rapeseed oil is the dominant feedstock
 524 for EU biodiesel production, constituting 39% of total production in 2018 (Phillips et al., 2019).
 525 The GHG emissions generated from rapeseed biodiesel produced via esterification was reported by
 526 Pehnelt and Vietze (2012), whose study excluded emissions from the transportation of the biodiesel
 527 product to the consumer, biodiesel combustion and waste treatment. A functional unit of 1 tonne of
 528 biodiesel production was used. Adopting identical system boundaries and functional unit, the GHG
 529 emissions generated by biodiesel production was calculated by summing the emissions from SCG
 530 collection, Organosolv pre-treatment and transesterification. For the collection and pre-treatment,
 531 the GHG emissions generated from biodiesel production were calculated using Equation (15),
 532 where ‘Process GHG’ refers to the total GHG emissions of each process.

$$\text{GHG from biodiesel production} = \text{Process GHG} \times \frac{\text{Biodiesel revenue}}{\text{Total revenue}} \quad (15)$$

533

534 The GHG emissions of the scenarios were compared against that of rapeseed biodiesel as shown in
 535 Figure 4 (e). The GHG emissions in Scenario C (1900 kg CO₂-eq./t biodiesel) are 29% lower than
 536 that of Scenario B (2678 kg CO₂-eq./t biodiesel) as it excludes transportation of the 23.8 tonnes of
 537 SCG required to produce 1 tonne of biodiesel. Besides that, Scenarios C and D produce GHG
 538 emissions that are 13% and 17% lower than rapeseed biodiesel.

539 The relatively low emissions of Scenario D are due to the exclusion of waste treatment emissions
 540 (which constitute 18% of total GHG emissions/t SCG) and use of Equation (15) (as biodiesel
 541 revenue represents just 7% of total revenue). Although the GHG emissions/t biodiesel appear
 542 promisingly low, Figure 4 (d) shows that total GHG emissions generated by Scenario D are 7 times
 543 greater than the emissions credited from displacing the use of conventional products. Thus,
 544 producing these high-value chemicals (e.g., vanillin, PHB) via the SCG biorefinery results in
 545 greater GHG emissions than conventional production methods.

546 According to the IEA, the production cost of conventional biodiesel ranges from 0.66–0.86 £/L
547 (International Energy Agency, 2012). All the scenarios apart from Scenario A result in biodiesel
548 production costs that are within this range. The results from this comparison indicate that SCG
549 biorefineries could potentially be used to meet growing biodiesel demands.

550 **4.3 Insights and Recommendations**

551 From the economic and environmental evaluations performed in Section 4.2, Scenario C was found
552 to be the most promising SCG biorefinery strategy. Although its *NPV* of £3.1 million is around 5
553 times lower than that of Scenario D, its GHG emissions (79 kg CO₂-eq./t SCG processed or 1900 kg
554 CO₂-eq./t biodiesel) are 28 times lower than Scenario D, 7 times lower than SCG landfilling (525
555 kg CO₂-eq./t SCG) and 13% lower than that of conventional rapeseed biodiesel (2191 kg CO₂-eq./t
556 biodiesel). It also has a biodiesel cost of production of 0.72 £/L, which is within the range estimated
557 by IEA (0.66–0.86 £/L). Furthermore, a practical advantage of using SCG from a coffee factory is
558 a more consistent feedstock flowrate and composition than SCG from coffee establishments,
559 resulting in fewer changes in operating conditions and product output. However, the economic
560 viability of Scenario C is sensitive to product price fluctuations, with 55.6% and 33.3% likelihoods
561 of $\geq 0\%$ and $< -50\%$ economic risks, respectively (Figure 4 (c)). Nonetheless, a positive *EP* is
562 maintained for price fluctuations within 10% of the base price.

563 Theoretically, the supply of the net heat generated to heat networks would represent an opportunity
564 to further reduce the biorefinery's carbon emissions through application of carbon credits. However,
565 the Derbyshire coffee factory considered in this study is one of more than 20 Nestlé coffee factories
566 worldwide currently incinerating the SCG it produces to meet the factory's heat energy
567 requirements ("Grounds for sustainability: coffee for energy, fuel and a cleaner world," 2013).
568 Future studies on the valorisation of SCG from instant coffee factories must thus account for the
569 economic and environmental impact of diverting SCG to a biorefinery and away from combustion
570 to generate the heat requirements of the factory. Including this in the analysis would likely have
571 negative implications on both the economics and emissions of the SCG biorefinery. However, the

biorefinery strategy could still represent a more profitable method of utilising SCG waste than combustion. As size was found to be an important factor affecting the economic performance and risk of a SCG biorefinery, different coffee factory sizes should be explored in these studies.

Additionally, the environmental evaluations of this study only considered GHG emissions. The environmental performances of the scenarios may differ upon assessment of other categories such as acidification potential and human toxicity potential. Other environmental impact categories should also be evaluated in future studies for a more holistic view of SCG biorefinery environmental performance.

Oil extraction and PHB production were identified as the processes with the largest costs in Scenarios A and D (see Figure D.3 of Appendix D). *n*-hexane and cellulase represent 25% and 17% of the total annual costs of Scenarios A and D, respectively. Thus, further studies on biodiesel and PHB production from SCG should aim to reduce usage of *n*-hexane and cellulase to maximise potential cost reductions. The technologies used in Scenario C must also be scaled to pilot plant levels to verify technical feasibility of the SCG biorefinery strategy. The accuracy of this study's results depends heavily on the financial investments and engineering capability required to scale these processes up economically.

588

589 **5 Conclusions**

This study investigates the future prospects of SCG biorefineries by assessing four SCG biorefinery scenarios in terms of their economic and environmental performances. The parameters altered between scenarios include biorefinery size, design configuration and location relative to the SCG source. SCG was either obtained from London coffee establishments or a coffee factory in Derbyshire. Two biorefinery configurations were used, with one producing biodiesel and electricity (Configuration I) and the other biodiesel with a range of high-value chemicals (Configuration II).

Overall, the results of this study indicate that future SCG biorefineries are likely to be of large scale and located on the site of an instant coffee factory. Heightened growth in demand for advanced biofuels coupled with pressures to reduce factory emissions mean that the waste-to-fuel biorefinery pathway could be regarded as an economically and environmentally attractive additional value chain for coffee factories. Provided that the relevant technologies can be successfully scaled up, production of multiple high-value chemicals is likely to be incorporated into SCG biorefineries due to attractive economic returns. Implementation of sustainable on-site energy generation will be crucial to minimise the high GHG emissions of the plant. Finally, SCG biorefineries have the potential to meet growing biodiesel demand, with similar production costs and lower GHG emissions when compared to conventional biodiesel.

Acknowledgement

This work was supported by the UKRI Natural Environment Research Council (NE/R012938/1) through the UKRI/NERC Industrial Innovation Fellowship Programme.

References

- Abdelaziz, O.Y., Al-Rabiah, A.A., El-Halwagi, M.M., Hulteberg, C.P., 2020. Conceptual design of a kraft lignin biorefinery for the production of valuable chemicals via oxidative depolymerization. *ACS Sustainable Chemistry and Engineering*. 8, 8823–8829. <https://doi.org/10.1021/acssuschemeng.0c02945>
- Abdelaziz, O.Y., Ravi, K., Mittermeier, F., Meier, S., Riisager, A., Lidén, G., Hulteberg, C.P., 2019. Oxidative Depolymerization of Kraft Lignin for Microbial Conversion. *ACS Sustainable Chemistry and Engineering*. 7, 11640–11652. <https://doi.org/10.1021/acssuschemeng.9b01605>
- Al-Hamamre, Z., Foerster, S., Hartmann, F., Kröger, M., Kaltschmitt, M., 2012. Oil extracted from spent coffee grounds as a renewable source for fatty acid methyl ester manufacturing. *Fuel*. 96, 70–76. <https://doi.org/10.1016/j.fuel.2012.01.023>
- Allesina, G., Pedrazzi, S., Allegretti, F., Tartarini, P., 2017. Spent coffee grounds as heat source for coffee roasting plants: Experimental validation and case study. *Applied Thermal Engineering*. 126, 730-736. <https://doi.org/10.1016/j.applthermaleng.2017.07.202>
- Bio-bean, 2021. Coffee logs. <https://www.bio-bean.com/coffee-logs/> (accessed 17 May 2021)
- Caetano, N.S., Silva, V.F.M., Melo, A.C., Martins, A.A., Mata, T.M., 2014. Spent coffee grounds for biodiesel production and other applications. *Clean Technologies and Environmental Policy*.

16, 1423–1430. <https://doi.org/10.1007/s10098-014-0773-0>

Davis, R., Tao, L., Tan, E.C.D., Biddy, M.J., Beckham, G.T., Scarlata, C., Jacobson, J., Cafferty, K., Ross, J., Lukas, J., Knorr, D., Schoen, P., 2013. Process design and economics for the conversion of lignocellulosic biomass to hydrocarbons: dilute-acid and enzymatic deconstruction of biomass to sugars and biological conversion of sugars to hydrocarbons. www.nrel.gov/publications (accessed 7 May 2021).

Department for Environment, Food and Rural Affairs (DEFRA), the Department of Agriculture, Environment and Rural Affairs (DAERA), the Welsh Government and the Scottish Government, 2020. Circular economy package policy statement. <https://www.gov.uk/government/publications/circular-economy-package-policy-statement/circular-economy-package-policy-statement> (accessed 18 May 2021).

Efthymiopoulos, I., Hellier, P., Ladommatos, N., Russo-Profil, A., Eveleigh, A., Aliev, A., Kay, A., Mills-Lamptey, B., 2018. Influence of solvent selection and extraction temperature on yield and composition of lipids extracted from spent coffee grounds. *Industrial Crops and Products*. 119, 49–56. <https://doi.org/10.1016/j.indcrop.2018.04.008>

Fujita, I., Wada, K., 2008. A process for producing succinic acid. WO2008010373. <https://patentscope.wipo.int/search/en/detail.jsf?docId=WO2008010373&tab=PCTBIBLIO> (accessed 14 April 2021)

Giller, C., Malkani, B., Parasar, J., 2017. Coffee to Biofuels. Senior Design Reports (CBE). 94. University of Pennsylvania. https://repository.upenn.edu/cbe_sdr/94/ (accessed 11 April 2021).

Gómez-Ríos, D., Navarro, G., Monsalve, P., Barrera-Zapata, R., Ríos-Estapa, R., 2019. Aspen plus simulation strategies applied to the study of chitin ioextraction from shrimp waste. *Food Technology and Biotechnology*. 57, 238–248. <https://doi.org/10.17113/ftb.57.02.19.6003>

Guardian, 2013. Grounds for sustainability: coffee for energy, fuel and a cleaner world. <https://www.theguardian.com/sustainable-business/grounds-sustainability-coffee-energy-fuel-pollution> (accessed 16 May 2021).

Hochegger, M., Cottyn-Boitte, B., Cézard, L., Schober, S., Mittelbach, M., Li, H., 2019. Influence of Ethanol Organosolv Pulping Conditions on Physicochemical Lignin Properties of European Larch. *International Journal of Chemical Engineering*. 2019, 1734507. <https://doi.org/10.1155/2019/1734507>

Humbird, D., Davis, R., Tao, L., Kinchin, C., Hsu, D., Aden, A., Schoen, P., Lukas, J., Olthof, B., Worley, M., Sexton, D., Dudgeon, D., 2011. Process Design and Economics for Biochemical Conversion of Lignocellulosic Biomass to Ethanol: Dilute-Acid Pretreatment and Enzymatic Hydrolysis of Corn Stover. <https://doi.org/10.2172/1013269>

IEA Bioenergy, 2021. Fossil and biogenic carbon emissions. <https://www.ieabioenergy.com/iea-publications/faq/woodybiomass/biogenic-co2/> (accessed 14 May 2021).

International Energy Agency, 2012. World Energy Outlook 2012. <https://www.iea.org/reports/world-energy-outlook-2012> (accessed 7 May 2021).

International Organization for Standardization, 2018. ISO 14067:2018, Carbon footprint of products. <https://www.iso.org/obp/ui/#iso:std:iso:14067:ed-1:v1:en> (accessed 15 May 2021).

Kang, S.B., Oh, H.Y., Kim, J.J., Choi, K.S., 2017. Characteristics of spent coffee ground as a fuel and combustion test in a small boiler (6.5 kW). *Renewable Energy*. 113, 1208–1214. <https://doi.org/10.1016/j.renene.2017.06.092>

Karmee, S.K., 2018. A spent coffee grounds based biorefinery for the production of biofuels, biopolymers, antioxidants and biocomposites. *Waste Management*. 72, 240–254. <https://doi.org/10.1016/j.wasman.2017.10.042>

Kondamudi, N., Mohapatra, S.K., Misra, M., 2008. Spent Coffee Grounds as a Versatile Source of Green Energy. *Journal of Agricultural and Food Chemistry*. 56, 11757–11760. <https://doi.org/10.1021/jf802487s>

Kookos, I. K., 2018. Technoeconomic and environmental assessment of a process for biodiesel production from spent coffee grounds (SCGs). *Resources, Conservation and Recycling*. 134, 156–164. <https://doi.org/10.1016/j.resconrec.2018.02.002>

- 681 Kourmentza, C., Economou, C.N., Tsafrakidou, P., Kornaros, M., 2018. Spent coffee grounds make
682 much more than waste: Exploring recent advances and future exploitation strategies for the
683 valorization of an emerging food waste stream. *Journal of Cleaner Production*. 172, 980–992.
684 <https://doi.org/10.1016/j.jclepro.2017.10.088>
- 685 Lee, M., Yang, M., Choi, S., Shin, J., Park, C., Cho, S.K., Kim, Y.M., 2019. Sequential production
686 of lignin, fatty acid methyl esters and biogas from spent coffee grounds via an integrated
687 physicochemical and biological process. *Energies*. 12, 2360.
688 <https://doi.org/10.3390/en12122360>
- 689 Li, Q., Xing, J., Li, W., Liu, Q., Su, Z., 2009. Separation of Succinic Acid from Fermentation Broth
690 Using Weak Alkaline Anion Exchange Adsorbents. *Industrial and Engineering Chemistry*
691 *Research*. 48, 3595–3599. <https://doi.org/10.1021/ie801304k>
- 692 Limousy, L., Jeguirim, M., Dutournié, P., Kraiem, N., Lajili, M., Said, R., 2012. Gaseous products
693 and particulate matter emissions of biomass residential boiler fired with spent coffee grounds
694 pellets. *Fuel*. 107, 323–329. <https://doi.org/10.1016/j.fuel.2012.10.019>
- 695 Martinez-Saez, N., García, A.T., Pérez, I.D., Rebollo-Hernanz, M., Mesías, M., Morales, F.J.,
696 Martín-Cabrejas, M.A., del Castillo, M.D., 2017. Use of spent coffee grounds as food
697 ingredient in bakery products. *Food Chemistry*. 216, 114–122.
698 <https://doi.org/10.1016/j.foodchem.2016.07.173>
- 699 Massaya, J., Prates Pereira, A., Mills-Lamptey, B., Benjamin, J., Chuck, C.J., 2019.
700 Conceptualization of a spent coffee grounds biorefinery: A review of existing valorisation
701 approaches. *Food and Bioproducts Processing*. 118, 149–166.
702 <https://doi.org/10.1016/j.fbp.2019.08.010>
- 703 Mata, T.M., Martins, A.A., Caetano, N.S., 2018. Bio-refinery approach for spent coffee grounds
704 valorization. *Bioresource Technology*. <https://doi.org/10.1016/j.biortech.2017.09.106>
- 705 Mayson, S., Williams, I.D., 2021. Applying a circular economy approach to valorize spent coffee
706 grounds. *Resources, Conservation and Recycling*. 172, 105659.
707 <https://doi.org/10.1016/j.resconrec.2021.105659>
- 708 McNutt, J., He, Q., 2018. Spent coffee grounds: A review on current utilization. *Journal of*
709 *Industrial and Engineering Chemistry*. 71, 78–88. <https://doi.org/10.1016/j.jiec.2018.11.054>
- 710 Mussatto, S.I., Carneiro, L.M., Silva, J.P.A., Roberto, I.C., Teixeira, J.A., 2011. A study on
711 chemical constituents and sugars extraction from spent coffee grounds. *Carbohydrate*
712 *Polymers*. 83, 368–374. <https://doi.org/10.1016/j.carbpol.2010.07.063>
- 713 Najdanovic-Visak, V., Lee, F.Y.L., Tavares, M.T., Armstrong, A., 2017. Kinetics of extraction and
714 in situ transesterification of oils from spent coffee grounds. *Journal of Environmental*
715 *Chemical Engineering*. 5, 2611–2616. <https://doi.org/10.1016/j.jece.2017.04.041>
- 716 Ng, D.K.S., Ng, K.S., Ng, R.T.L., 2017. Integrated biorefineries, in: Abraham, M.A. (Eds.),
717 *Encyclopedia of Sustainable Technologies*. Elsevier, Oxford, pp. 299–314.
- 718
- 719 Ng, K.S., Martinez-Hernandez, E., 2020. Techno-economic assessment of an integrated bio-oil
720 steam reforming and hydrodeoxygenation system for polygeneration of hydrogen, chemicals,
721 and combined heat and power production, in: Ren, J., Wang, Y., He, C. (Eds), *Towards*
722 *Sustainable Chemical Processes*. Elsevier, Oxford, pp. 69–98
723
- 724 Ng, K.S., Yang, A., Yakovleva, N., 2019. Sustainable waste management through synergistic
725 utilisation of commercial and domestic organic waste for efficient resource recovery and
726 valorisation in the UK. *Journal of Cleaner Production*. 227, 248–262.
727 <https://doi.org/10.1016/j.jclepro.2019.04.136>
- 728 Ng, K.S., Zhang, N., Sadhukhan, J., 2013. Techno-economic analysis of polygeneration systems
729 with carbon capture and storage and CO₂ reuse. *Chemical Engineering Journal*. 219, 96–108.
730 <https://doi.org/10.1016/j.cej.2012.12.082>
- 731 Nieder-Heitmann, M., Haigh, K., Görgens, J.F., 2019. Process design and economic evaluation of
732 integrated, multi-product biorefineries for the co-production of bio-energy, succinic acid, and

- polyhydroxybutyrate (PHB) from sugarcane bagasse and trash lignocelluloses. *Biofuels, Bioproducts and Biorefining* 13, 599–617. <https://doi.org/10.1002/bbb.1972>
- Obruca, S., Benesova, P., Kucera, D., Petrik, S., Marova, I., 2015. Biotechnological conversion of spent coffee grounds into polyhydroxyalkanoates and carotenoids. *New Biotechnology*. 32, 569–574. <https://doi.org/10.1016/j.nbt.2015.02.008>
- Panusa, A., Zuorro, A., Lavecchia, R., Marrosu, G., Petrucci, R., 2013. Recovery of natural antioxidants from spent coffee grounds. *Journal of Agricultural and Food Chemistry*. 61, 4162–4168. <https://doi.org/10.1021/jf4005719>
- Park, J., Kim, B., Lee, J.W., 2016. In-situ transesterification of wet spent coffee grounds for sustainable biodiesel production. *Bioresource Technology*. 221, 55–60. <https://doi.org/10.1016/j.biortech.2016.09.001>
- Phillips, S., Flach, B., Lieberz, S., Bolla, S., 2019. USDA EU Biofuels Annual. <https://www.fas.usda.gov/data/eu-28-biofuels-annual-1> (accessed 15 March 2021).
- Recycling Magazine, 2019. Reducing coffee waste. <https://www.recycling-magazine.com/2019/10/01/reducing-coffee-waste/> (accessed 21 April 2021).
- Rivera, X.C.S., Gallego-Schmid, A., Najdanovic-Visak, V., Azapagic, A., 2020. Life cycle environmental sustainability of valorisation routes for spent coffee grounds: From waste to resources. *Resources, Conservation and Recycling*. 157, 104751. <https://doi.org/10.1016/j.resconrec.2020.104751>
- Sadhukhan, J., Ng, K.S., Hernandez, E.M., 2014. *Biorefineries and chemical processes : design, integration and sustainability analysis*, Ebook central. John Wiley & Sons Ltd, Chichester.
- Saratale, G., Bhosale, R., Shobana, S., Rajesh Banu, J., Pugazhendhi, A., Mahmoud, E., Sirohi, R., Kant Bhatia, S., Atabani, A.E., Mulone, V., Yoon, J.-J., Shin, H.S., Kumar, G., 2020. A review on valorization of spent coffee grounds (SCG) towards biopolymers and biocatalysts production. *Bioresource Technology*. 314, 123800. <https://doi.org/10.1016/j.biortech.2020.123800>
- Somnuk, K., Eawlex, P., Prateepchaikul, G., 2017. Optimization of coffee oil extraction from spent coffee grounds using four solvents and prototype-scale extraction using circulation process. *Agriculture and Natural Resources*. 51, 181–189. <https://doi.org/10.1016/j.anres.2017.01.003>
- Thoppil, Y., Zein, S.H., 2021. Techno-economic analysis and feasibility of industrial-scale biodiesel production from spent coffee grounds. *Journal of Cleaner Production*. 307, 127113. <https://doi.org/10.1016/j.jclepro.2021.127113>
- Trejo-Zárraga, F., Hernández-Loyo, F. de J., Chavarría-Hernández, J.C., Sotelo-Boyás, R., 2018. Kinetics of Transesterification Processes for Biodiesel Production, in: *Biofuels - State of Development*. IntechOpen, pp. 149–179. <https://doi.org/10.5772/intechopen.75927>
- Tsoutsos, T., Tournaki, S., Gkouskos, Z., Paraíba, O., Giglio, F., García, P.Q., Braga, J., Adrianos, H., Filice, M., 2019. Quality characteristics of biodiesel produced from used cooking oil in Southern Europe. *ChemEngineering* 3, 1–13. <https://doi.org/10.3390/chemengineering3010019>
- Tuntiwiwattanapun, N., Monono, E., Wiesenborn, D., Tongcumpou, C., 2017. In-situ transesterification process for biodiesel production using spent coffee grounds from the instant coffee industry. *Industrial Crops and Products*. 102, 23–31. <https://doi.org/10.1016/j.indcrop.2017.03.019>
- van Ree, R., de Jong, E., Kwant, K., 2012. Bio-based chemicals: value added products from biorefineries. <https://www.ieabioenergy.com/blog/publications/bio-based-chemicals-value-added-products-from-biorefineries/> (accessed 7 May 2021).
- Zetterholm, J., Bryngemark, E., Ahlström, J., Söderholm, P., Harvey, S., Wetterlund, E., 2020. Economic Evaluation of Large-Scale Biorefinery Deployment: A Framework Integrating Dynamic Biomass Market and Techno-Economic Models. *Sustainability*. 12, 7126. <https://doi.org/10.3390/su12177126>